

INVESTIGATIONS ON RAILWAY TRACKS WITH SPECIAL EMPHASIS ON PARTIALLY UNSUPPORTED SLEEPERS DUE TO VOIDS

R. L A M M E R I N G and M. P L E N G E

INSTITUTE OF MECHANICS, UNIVERSITY OF THE FEDERAL ARMED FORCES

22039 Hamburg, Germany

A single sleeper, two adjacent sleepers and a track segment are investigated experimentally in order to get a basic knowledge of the dynamic response of a vertically loaded railway track up to 800 Hz. Since voids are often observed between sleepers and the underlying ballast, special emphasis is laid on investigations of partially unsupported sleepers. Detailed information on the dynamic displacement field is obtained by the holographic interferometry which is used beside conventional accelerometers to record the oscillations. The results show that deviations from optimal coupling to the ground result in significant changes of the dynamic behavior.

1. INTRODUCTION

The rapid development of modern railway systems, characterized by increasing travelling speeds and axle loads, requires to consider the components as a whole and, especially, to take into account the interaction between them, e.g. between the vehicle, track, and subsoil.

In the last 20 years, much effort has been made to develop mathematical models in order to understand and to solve various practical problems, cf. KNOTHE and GRASSIE [7], and POPP and SCHIEHLEN [11]. A lot of scientific work has been performed to refine mechanical models of the bogie-wheelset-track system, e.g. by RIPKE and KNOTHE [9]. However, even in sophisticated models, the subsoil is often represented simply by a spring and a damper connected in parallel. This mechanical model must be considered as insufficient for a detailed investigation on the dynamic response of a railway track at high dynamic loading. Therefore, the commonly used multi-body dynamic computer codes are not well suited for the analysis of the entire system, since the subsoil is not modelled accurately.

On the other hand, accurate models of the subsoil have been developed for various other applications, e.g. by GAUL and PLENGE [4, 5] and WOLF [12] for rigid and elastic foundations. The interaction between adjacent rigid foundations has also been considered by GAUL and PLENGE [4]. In [3], AUERSCH presents the determination of subsoil properties from wave propagation and refers directly to the rail traffic.

Until now, only little work has been done that aims at the interaction between the subsoil and the railway track or its constituents, e.g. sleepers, adjacent sleepers, and systems of sleepers connected by rails. In [2], AUERSCH *et al.* present numerical results of rigid sleepers resting on an elastic half-space under the assumption of a linear-elastic material behavior. The coupling between adjacent sleepers through the subsoil is considered experimentally by RÜCKER [10], AUERSCH *et al.* [1] and by PRANGE *et al.* [8]. During in situ measurements, the rail was removed from the sleepers and excitation of the sleepers was performed. However, these experiments cannot be considered to be sufficient for the verification of new analysis models. The interaction of adjacent sleepers and the interaction between the sleeper rail system and the subsoil still requires further experimental research.

This is the starting point of the present paper. In laboratory experiments, the dynamic behavior of a single sleeper is investigated. Moreover, the interaction between sleepers which are coupled through the subsoil is examined. Further investigations focus on voided sleepers, i.e. sleepers separated by a gap from the underlying subsoil. These gaps develop during operation and can be considered as long-term damages. The results show the effect of these gaps on the short-term dynamics. For a pointwise analysis of the dynamic response of the sleepers and the rails, piezoelectric accelerometers and a laser vibrometer are used. Further insight is provided by means of the holographic interferometry which is used to present the entire displacement field. The frequency range under consideration is up to 800 Hz, thus taking into account e.g. the relatively short wavelength irregularities of the rail and polygonalized wheels beside the regular vertical excitations.

2. EXPERIMENTAL SET-UP

The experimental investigations presented in this paper are performed in a laboratory in which an excavation of the dimensions 4.0 m × 4.0 m × 2.0 m is filled with a test soil. Undisturbed soil is directly bordering the test soil without any walls so that almost any impedance difference is avoided. Therefore, even low frequency waves with a high wavelength may propagate without reflections. The

test soil is a mixture of sand and fine gravel with the properties shown in Table 1. This testbed allows for investigations on full-scale track segments consisting of up to five concrete sleepers B70W60 linked with rails UIC60 that are commonly used for ballasted German high-speed railway tracks.

Table 1. Properties of the soil and the sleeper.

Object	Property	Data
soil	shear wave velocity	149 m/s
	density	1926.5 kg/m ³
	Poisson's ratio	0.12
sleeper	length	2600 mm
	width	225 mm – 300 mm
	height	176 mm – 230 mm
	mass	304 kg

For the loading of the track segment and its constituents, it is necessary to apply static as well as dynamic forces. Two pneumatic cylinders supported by a crossbeam generate a static load of 10 kN each. This load is about one tenth of the operating load, but our own experience (see Sec. 3.3) as well as investigations made e.g. by WU and THOMPSON [13] show that a small static load influences the dynamic behavior of the system significantly but that a further loading causes only little modifications. The dynamic loads are applied by an electrodynamic shaker, the force amplitude of which is amplified by a lever mechanism.

The dynamic behavior of the structure under investigation is realized by piezoelectric accelerometers and by a laser vibrometer as well as by holographic interferometry. The accelerometers and the vibrometer allow for the collection of time signals at specific locations, whereas the holographic interferometry is an appropriate tool to measure the displacement field of an oscillating surface.

The basic principles of the holographic interferometry is outlined as follows. A beam of coherent light emitted by a laser is divided into two waves by a beamsplitter. Each narrow ray bundle is then expanded by a lens or a system of lenses. The reference wave is directly guided onto a photosensitive plate of high resolution. The object wave is reflected by the surface of an opaque object and both waves interfere on the hologram plate in such a way that the variation of the relative phase from point to point is transformed into an interference pattern retaining the complete information of the object. The interference pattern is decoded by illuminating the hologram plate by the reference light and the virtual 3D-image of the object is obtained.

In order to record the displacement field, the holographic film is exposed twice at a very short time interval. During this period of time, the wave under

consideration is propagating and the difference of the surface shapes is recorded on the film. Reconstruction of the hologram by reference light shows both images of the object at the same time. The object is covered by light and dark interference fringes that represent contour lines of the deformation. More details are given by GAUL and PLENGE in [5].

3. IDENTIFICATION OF THE CONCRETE SLEEPER B70W60

3.1. Scope of experimental investigations

Before starting the experimental investigations on a track segment, a detailed program is performed in order to identify the eigenfrequencies and modes of the concrete sleeper B70W60 which is widely used on German railway tracks. Various boundary conditions are realized: free-free, perfectly coupled to the soil and hovering ends. A hovering end of a sleeper arises when a gap between the soil and the sleeper grows during operation. The gap may be built either at one end of the sleeper or at both ends. In the latter case, the contact between the sleeper and the subsoil exists only in the middle of the sleeper. Both situations are depicted in Fig. 1. As mentioned above, the frequency range under consideration is up to 800 Hz.

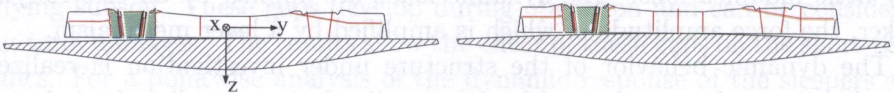


FIG. 1. Voided sleepers.

3.2. Sleeper with free-free boundary conditions

In order to realize the free-free boundary conditions and to exclude the influence of the support in the following investigations, the concrete sleeper is rotated with respect to its axis by 90° and suspended by two ropes. The excitation is performed horizontally (i.e. in the rotated z -direction) at one end by an electrodynamic shaker. The positions of the shaker and the accelerometers as well as the frequency response function are shown in Fig. 2.

From there it can be seen that the frequency response function is characterized by narrow peaks of bending modes with respect to the x -axis. In Fig. 2, the peaks are labelled with the corresponding modes. Beyond that, particular accelerometers give rise to additional peaks, e.g. at 52.5 Hz and at 760 Hz. At 52.5 Hz, the torsional mode is excited as a result of an imperfection in the ex-

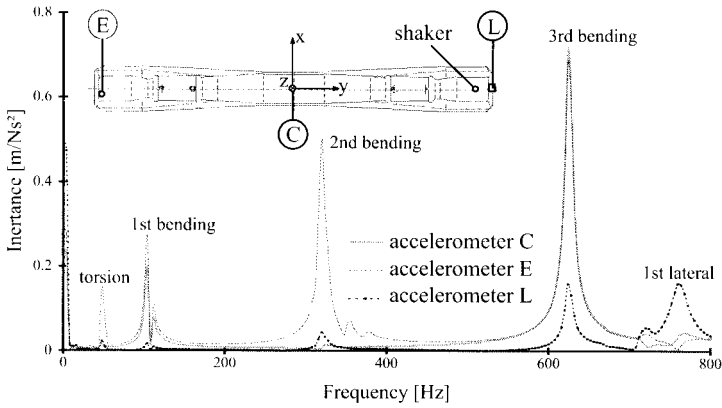


FIG. 2. Frequency response function of the rotated and horizontally excited sleeper.

perimental set-up and observed by the accelerometer E that is mounted opposite to the shaker position with an offset from the center axis, cf. Fig. 2. At about 760 Hz, the first longitudinal mode of the sleeper occurs which would result in a lateral vibration of the track.

The experiment was repeated with the same sleeper which again was suspended but not rotated. Again, the sleeper is excited horizontally, i.e. in the x-direction. The results are shown in Fig. 3 showing the bending modes with respect to the z-axis. The frequency response function is similar to that shown in Fig. 2. The first three bending modes can clearly be identified, however, they are shifted towards the higher frequencies. The longitudinal mode at 760 Hz is not observed by a sensor on the top surface of the sleeper head (not shown in Fig. 3).

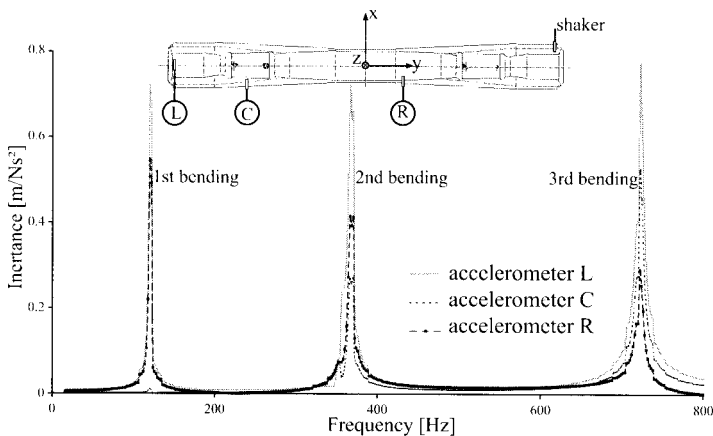


FIG. 3. Frequency response function of the horizontally excited sleeper.

3.3. Ideal contact between sleeper and subsoil

Next, the sleeper is laid on the test soil and perfectly coupled with the ground. Optimal coupling conditions are achieved by a plaster on which the sleeper is placed after it is spread on the soil in the contact area. Various tests were performed in which the static load and the direction of excitation (vertical, lateral and tilt) were varied among other. From the frequency response functions those frequencies were identified by which the system is substantially affected. At these frequencies, the displacement field of the soil and the sleeper is recorded by use of the holographic interferometry.

Figure 4 shows the frequency response function as well as the locations of the shaker and the accelerometers. The experiments were performed without any static load. From the signals it can be seen that the sleeper undergoes especially bending oscillations. The first bending mode is identified at approximately 128 Hz, and the third one at 632 Hz. Due to the elastic foundation of the sleeper, these frequencies are shifted to higher frequencies compared to the situation in Fig. 2. Furthermore, the amplitudes decrease significantly and reach only app. 20% of those in Fig. 2. Even modes do not occur due to the symmetric support and the symmetric excitation. It should be noticed that a lateral vibration is again recorded at 756 Hz.

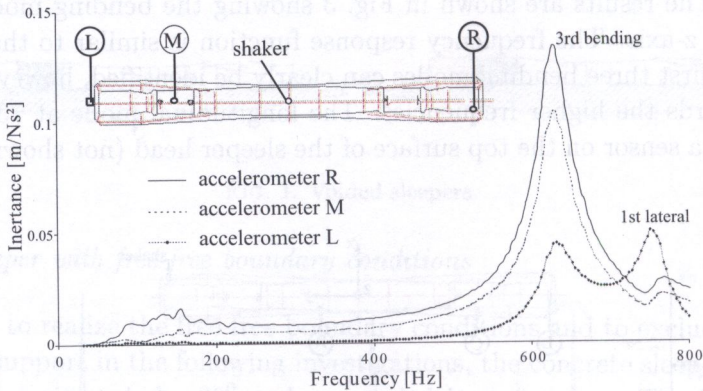


FIG. 4. Frequency response function of the ideally coupled sleeper.

The influence of the static load that is applied at the railseat area is shown in Fig. 5. The load is increased in steps of 2.5 kN up to 10 kN. It is obvious that the first load step results in a stronger coupling of the sleeper to the soil, so that especially the third bending mode is less developed. On the other hand, the frequency response function is almost not affected between the first and third bending mode. Below 110 Hz, any increase of the static load produces stiffening

of the system. These results are in good agreement with investigations of WU and THOMPSON [13] on a ballasted track. They report that an increase of the static load from 1.2 kN to 11 kN gives rise to the stiffness (factor 2.4) at a dynamic excitation at 50 Hz, but that further doubling of the load increases the stiffness by 5% only.

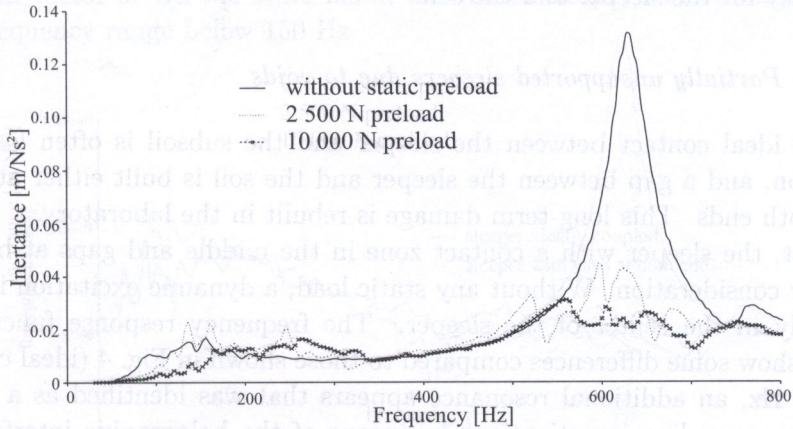


FIG. 5. Influence of the static preload on the frequency response function of an ideally coupled sleeper.

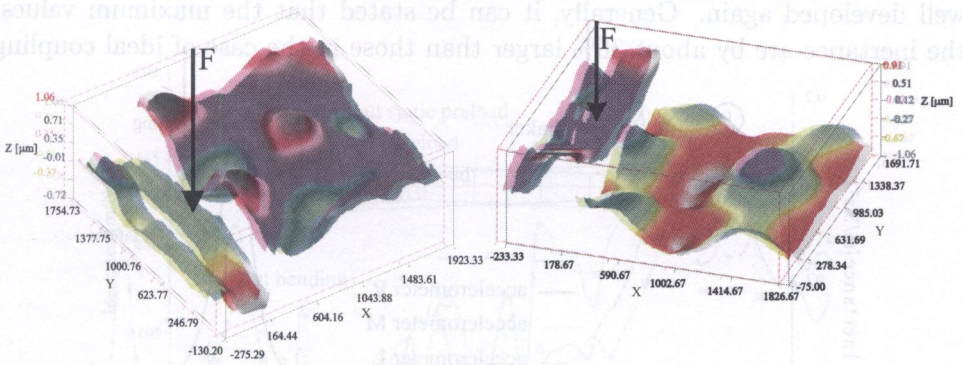


FIG. 6. Dynamic displacement fields of the soil and the sleeper in the case of ideal coupling and excitation in the sleeper center at 148 Hz. The phase difference between both figures is 180° .

From the experiments above, the frequency of 148 Hz is selected for further investigations focussing on the oscillations of the sleeper and the wave propagation in the soil. Figure 6 shows the displacement field of the sleeper and the soil for two different phases that are shifted by 180° . The vibration of the sleeper can clearly be identified as the first bending mode. Furthermore, it is visible that the wave propagation in the soil starts at both contact areas between the sleeper and

soil. At 148 Hz, the wavelength is about 1 m, so there is a shear wave velocity of about 149 m/s in the soil. This result is in good agreement with seismic measurements. It should be noted that the interferogram was subdivided into two parts before the evaluation is started since the edge of the sleeper or shadows can influence the evaluation algorithm. Therefore, the displacement field is evaluated separately for the sleeper and the soil.

3.4. Partially unsupported sleepers due to voids

The ideal contact between the sleeper and the subsoil is often lost during operation, and a gap between the sleeper and the soil is built either at one end or at both ends. This long-term damage is rebuilt in the laboratory.

First, the sleeper with a contact zone in the middle and gaps at both ends is under consideration. Without any static load, a dynamic excitation is applied vertically in the center of the sleeper. The frequency response functions (cf. Fig. 7) show some differences compared to those shown in Fig. 4 (ideal coupling). At 52.5 Hz, an additional resonance appears that was identified as a torsional mode in succeeding investigations by means of the holographic interferometry. Due to the stiff coupling in the center of the sleeper, the first bending mode is difficult to excite and strongly damped. The peaks indicating the third bending mode and the lateral oscillation appear at nearly the same frequencies and are well developed again. Generally, it can be stated that the maximum values of the inertance are by about 30% larger than those in the case of ideal coupling.

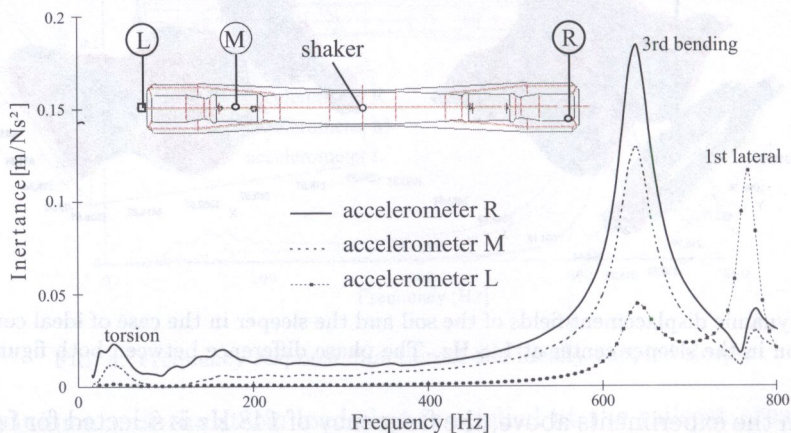


FIG. 7. Frequency response function of a sleeper coupled to the subsoil in its middle and hovering at both ends.

The receptances of the ideally coupled and voided sleepers are compared in Fig. 8. For this purpose, a static load of 10 kN is applied at the rail positions

and a dynamic load is introduced at the center. The signal of the accelerometer attached at the upper side of the sleeper head is shown as well as the corresponding signal from the ideally coupled sleeper. It is visible that both curves are in good agreement beyond 150 Hz. With the exception of a small frequency band at app. 440 Hz at which a kind of anti-resonance appears, the difference does not exceed the factor 2. On the other hand, the voided sleeper behaves much softer in the frequency range below 150 Hz.

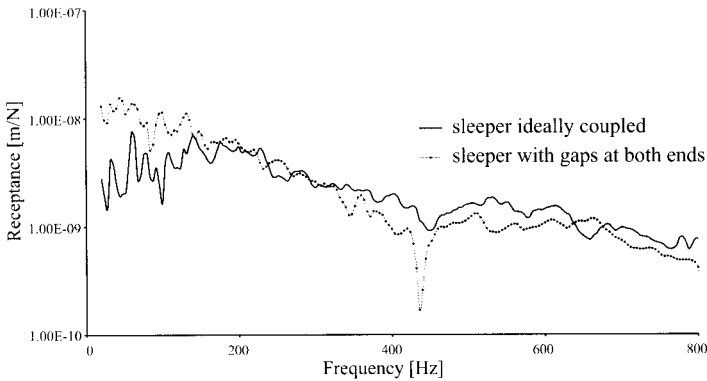


FIG. 8. Comparison of the receptances of the ideally coupled sleeper and a sleeper with gaps as both ends. 10 kN static load at each rail.

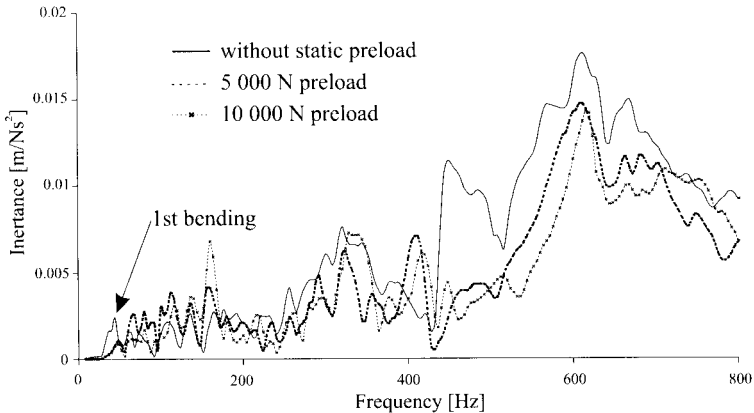


FIG. 9. The influence of the static preload on the frequency response function of a sleeper with one hovering end.

The next investigations aim at a sleeper which is well coupled to the subsoil at one end and hovering at the other end. Among others, the results in Fig. 9 were obtained showing the inertance at the hovering end as a function of frequency

and static load. Again, it is visible that the first load steps have a significant influence on the dynamic behavior whereas further load steps do not result in considerable modifications. At 40.5 Hz, the first bending mode is observed and the hovering end behaves like a cantilever. Higher preloads cause an amplitude reduction and a shift of the first eigenfrequency towards higher values. With increasing frequencies, the sleeper behavior is not uniform: up to 250 Hz, the system becomes softer; beyond 250 Hz, a stiffening effect due to the static load is observed. It should be noted that the static load improves the contact between the sleeper and the soil and, as a consequence of the changing boundary conditions, the underlying system is changed.

4. TWO ADJACENT SLEEPERS AND TRACK SEGMENT

4.1. Structural dynamics of two adjacent sleepers

The ideally coupled sleeper is now supplemented by a neighboring sleeper which is coupled to the subsoil in the middle and which hovers at both ends. The first one is excited vertically in its center by an electrodynamic shaker and the static preload is chosen up to 10 kN at each railseat area. The adjacent sleeper remains unloaded but is excited by waves spreading out from the excited sleeper. Accelerometers are mounted at both sleepers in order to investigate the dynamic behavior of this configuration.

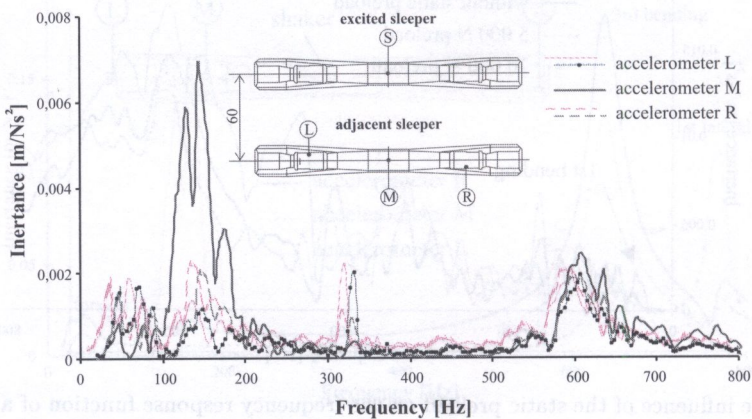


FIG. 10. Frequency response function of the adjacent sleeper with hovering ends.

The feedback of the adjacent sleeper on the dynamic behavior of the loaded sleeper is rather small, so that the resulting frequency response functions of the

excited sleeper are not shown here for the sake of brevity and since they are very similar to those in Figs. 4 and 5. At the adjacent sleeper, various eigenmodes are observed, some of which are well developed due to the imperfect coupling to the subsoil. The known bending modes at 148 Hz, 332 Hz and 608 Hz can easily be identified from Fig. 10; moreover, a rocking mode with respect to the sleeper axis at 45 Hz (cf. Fig. 11) and a torsion mode at 72 Hz are observed. In the contact area, the inertance reaches its maximum. The static preload does not significantly influence the frequency response function.

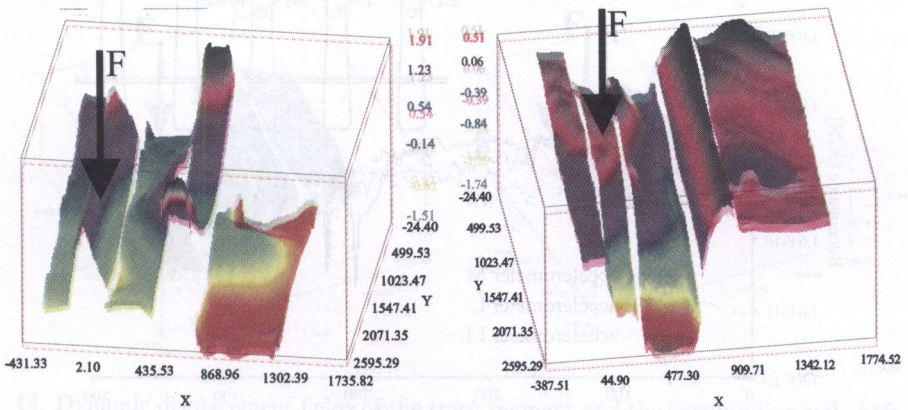


FIG. 11. Dynamic displacement fields of the two sleepers and the soil. The excitation frequency is 45 Hz.

Deeper insight into the dynamic response of the system is given by Fig. 11. From the displacement field on the left-hand side, the coupling conditions can easily be detected. The waves spread out from both ends of the loaded sleeper and from the center of the passive one. Here, the loaded sleeper is tilted whereas the passive one is bent. The displacement field in the figure on the right-hand side exhibits a phase difference and shows a tilted passive sleeper. The good coupling to the subsoil in its center is also obvious. Furthermore, it is visible that the loaded sleeper not only tilts but that this motion is superposed by a bending deformation. Obviously, an interaction between both sleepers takes place in the low frequency range.

4.2. Structural dynamics of a track segment

The following experiments are performed on a track segment consisting of five sleepers and two connecting rails. Both rails end in boxes filled with sand in order to avoid oscillations of the ends. Ten accelerometers and two force transducers are mounted in various patterns on the rails and the sleepers in order to record the

oscillations. One pattern was used to prove the symmetry of the response when the system is loaded symmetrically. The rail vibration is observed by another pattern, in which the accelerometers are mainly mounted on the top of the rails. Here, two places of excitation are chosen: on the sleeper and between the sleepers.

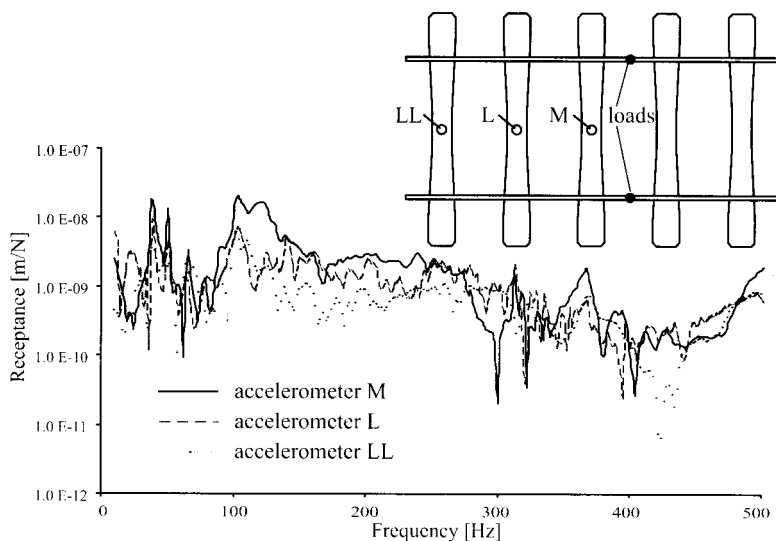


FIG. 12. Frequency response function of the track segment.

In the following, some results are presented which were obtained on a track segment which was ideally coupled to the underlying soil. The whole system is dynamically loaded by two forces acting vertically on both rails between the second and third sleeper. Both forces are applied in phase and 180° out of phase. The frequency response function which is presented in Fig. 12, is obtained when both forces are applied 180° out of phase to the rails. At frequencies of up to 100 Hz, the receptance at the center of the three sleepers observed is nearly the same, whereas in the frequency range from 100 Hz to 250 Hz the outer sleeper is generally showing the lowest receptance, and the sleeper in the middle the largest. The maximum value of the receptance is reached at 103 Hz. Here, the dynamic displacement field is observed by means of the holographic interferometry. In Fig. 13, the situation is shown for both cases, for the forces being out of phase and in phase. When the forces are in phase, the oscillations of the sleeper in the middle are associated with the first bending mode. Taking into account the additional mass of the rails, which causes the eigenfrequencies to decrease, this result is in good agreement with the frequency response functions in Fig. 4 (in which the first bending mode of the sleeper is identified at 128 Hz) and in Fig. 10

(in which also a clear peak is noticed at that frequency). Furthermore, it is clearly visible that the waves spread out from the rail in the middle of the track segment. On the right-hand side of Fig. 13, where the situation is shown when the forces are 180° out of phase, the displacement field of the sleeper and the surrounding soil is quite different. From the displacement field of the ground, it can clearly be seen that the forces are in counter-phase. This kind of excitation causes the sleeper in the middle to tilt.

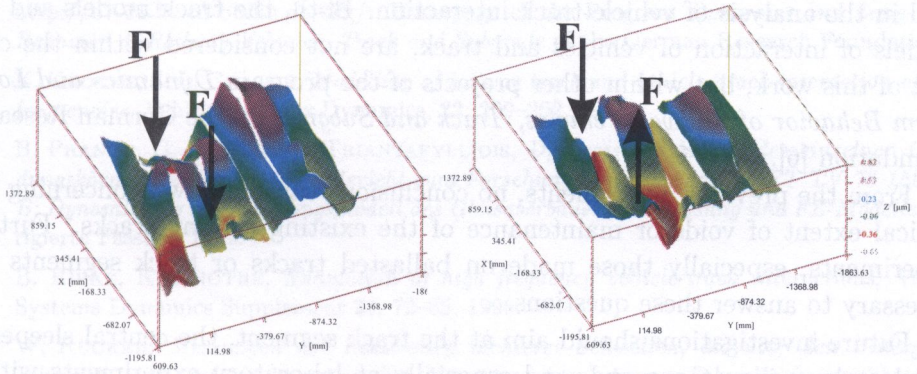


FIG. 13. Dynamic displacement fields of the track segment and the surrounding soil. Left-hand side: forces on both rails in phase. Right-hand side: forces in counter-phase.

5. CONCLUSIONS AND OUTLOOK

In this paper, the dynamic behavior of a single sleeper, two adjacent sleepers and a track segment is under consideration. Special emphasis is laid on the influence of voided sleepers on the short-term dynamics.

Investigations on a single sleeper show that a voided sleeper gives significant rise to the receptance at frequencies up to 150 Hz. Even in the case of vertical excitation, these boundary conditions allow for rigid body modes and torsional modes, which are not observed when the sleeper is perfectly coupled to the ground. At frequencies beyond 150 Hz, the dynamical behavior does not change significantly.

A static preload results in a stronger coupling of the sleeper to the ground and in stiffening of the system. Our own experiments confirm the observations made by WU and THOMPSON [13] who note that the main effect is already visible at comparatively small preloads.

Investigations of two adjacent sleepers and a track segment have shown that some of the characteristics which have been observed on a single sleeper, play also

an important role in the behavior of more complex structures. E.g., the same bending modes can be found not only in the frequency response functions of a single sleeper, but also in a system consisting of two adjacent sleepers and of a track segment.

Since the ideal coupling to the ground is inevitably lost during track operation, track models could be improved by taking into account the results of these laboratory experiments and by incorporating the effect of voided sleepers. Likewise, the increase of the receptance below 150 Hz are worth to be considered in the analysis of vehicle-track interaction. Both, the track models and the models of interaction of vehicles and track, are not considered within the context of this work, but within other projects of the program *Dynamics and Long-Term Behavior of Railway Vehicles, Track and Subgrade* of the German Research Foundation [6].

From the previous experiments, no conclusions can be drawn concerning the critical extent of voids or maintenance of the existing railway tracks. Further experiments, especially those made on ballasted tracks or track segments are necessary to answer these questions.

Future investigations should aim at the track segment, the central sleeper of which is hovering at one end, and especially at laboratory experiments with a ballasted track segment. The dynamic behavior of railway tracks under lateral loads will be another field of research in the near future. Furthermore, a comparison between the laboratory experiments presented above, the in situ experiments, and the numerical calculations will be performed.

ACKNOWLEDGEMENTS

The financial support of the German Research Foundation (Deutsche Forschungsgemeinschaft, DFG) within the program *Dynamics and Long-Term Behavior of Railway Vehicles, Track, and Subgrade* is gratefully acknowledged.

REFERENCES

1. L. AUERSCH, H.-L. HEBENER, W. RÜCKER, *Erschütterungen infolge Schienenverkehr: Theoretische und meßtechnische Untersuchungen zur Emission, zur Ausbreitung durch den Boden und zur Übertragung in Gebäude*, Bericht 19 zum BMFT-Vorhaben TV 8329, Verminderung des Verkehrslärms in Städten und Gemeinden - Teilprogramm Schienennahverkehr. STUVA Köln, BAM Berlin 1986.
2. L. AUERSCH, R. ROHRMANN, W. RÜCKER, S. SAID, *Fahrzeug-Fahrweg-Untergrund-Umgebung: theoretische, rechen- und meßtechnische Untersuchungen*, VDI Berichte 635, Dynamik fortschrittlicher Bahnsysteme, 59-87, 1987.

3. L. AUERSCH, *Wave propagation in layered soils: theoretical solution in wavenumber domain and experimental results of hammer and traffic excitation*, *Journal of Sound and Vibration*, **173**, 2, 233–264, 1994.
4. L. GAUL, M. PLENGE, *Baugrundeinflüsse auf das Schwingungsverhalten von Fundamenten*, VDI Berichte **1082**, Dämpfung und Nichtlinearität, 195–220, 1993.
5. L. GAUL, M. PLENGE, *Progress in 3-d BE-calculations and optoelectronic measurement of soil-structure-interaction*, Elsevier Applied Science, London, *Advanced Dynamic Analysis by BEM, Developments in Boundary Element Methods - 7*, P. K. BANERJEE, S. KOBAYASHI [Eds.], Chapter 10, 353–403, 1992.
6. <http://b7-01.bv.tu-berlin.de/dfg/>: Homepage of the Program *Dynamics and Long-Term Behavior of Railway Vehicles, Track and Subgrade* of the German Research Foundation.
7. K. KNOTHE, S. L. GRASSIE, *Modelling of railway track and vehicle/track interaction at high frequencies*, *Vehicle Systems Dynamics*, **22**, 209–262, 1993.
8. B. PRANGE, G. HUBER, Th. TRIANTAFYLIDIS, *Dynamisches Modell des einzelnen Gründungskörpers, 2. Technischer Bericht zum Forschungsvorhaben des BMFT TV 78 150 Teil B: Dynamisches Rückwirkungsmodell des Gleisoberbaus: Feldmessung und FE-Modelle*, korrigierte Fassung 1982.
9. B. RIPKE, K. KNOTHE, *Simulation of high frequency vehicle-track interactions*, *Vehicle Systems Dynamics Supplement* **24**, 72–85, 1995.
10. W. RÜCKER, *Messungen der Reaktionen mehrerer Schwellen, die über den Untergrund gekoppelt sind, infolge harmonischer Erregung einer starren Schwelle in verschiedenen Erregermoden*, *Technischer Bericht zum Meilenstein D4 des Vorhabens Rad/Schiene*, Förderungskennzeichen TV 7817 2, Bundesanstalt für Materialprüfung, Berlin 1980.
11. K. POPP, W. SCHIEHLEN, *Fahrzeugdynamik. Eine Einführung in die Dynamik des Systems Fahrzeug-Fahrweg*, B. G. Teubner, Stuttgart 1993.
12. J. P. WOLF, *Dynamic soil-structure interaction*, Prentice Hall, Englewood Cliffs 1985.
13. T. X. WU, D. J. THOMPSON, *The effects of local preload on the foundation stiffness and vertical vibration of railway track*, *Journal of Sound and Vibration*, **219**, 5, 881–904, 1999.

Received February 24, 2000.
